Journal of Cultural Heritage 1 (2000) 45–58

S1296-2074(99)00118-1/FLA

Investigation of the technology of historic mortars

Antonia Moropoulou*, Asterios Bakolas, Katerina Bisbikou

Department of Chemical Engineering, Materials Science and Engineering Sector,
National Technical University of Athens, Iroon Polytechniou 9, Athens 15780, Greece

Received 15 June 1998; accepted 30 July 1999

Abstract – Historical evidence on the use of mortars to meet several needs has existed for millennia. With reference to the characteristic historical periods of the city of Rhodes, mortar sampling was performed on historical constructions, masonry and architectural surfaces. In the present work the different mortar technologies are investigated aiming to answer questions regarding their finality, i.e. whether their differences arise mainly from the various historical periods of construction or from the purposes they had to serve, imparting to the mortars the properties required by their function in the structure. Mineralogical, chemical, physical and mechanical investigations have been performed on characteristic samples after gradation. The exponentially declining function of the ratio CO_2/H_2O structurally bound to the CO_2 content shows a continuous evolution of the kinetics governing the various mechanisms of carbonation of the binder or the formation of hydraulic components during setting, hardening and ageing of the mortars. The grouping of mortars in well-distinct 'hydraulic levels' is ascribed to the physico-chemical cohesion and adhesion bonds developed at the matrix and matrix/aggregate interfaces, respectively, allowing for the mortars to either bear continuous stresses and strains as joint mortars or provide compact impermeable renderings which harden even more on contact with water. Hence, parameters determining the diversification of the resulting mortar/matrix types concern the raw materials employed as binding materials and the production processing. © 1999 Éditions scientifiques et médicales Elsevier SAS

Keywords: historic mortars / Rhodes / mineralogical investigation / chemical physical investigation / mechanical investigation

1. Introduction

Historical evidence has existed for millennia on the use of mortars to meet several needs. Historical sources refer to the use of mortars as isolating lining materials in cisterns, wells, aqueducts, shafts and duct drains, as supporting materials for pavements and mosaics, as plasters on external and internal walls and as supporting materials for frescoes, as well as joint mortars of masonry structures. In the south-eastern Mediterranean and especially in the island of Rhodes, the craftsmanship of mortars flourished from the second millennium BC [1], showing glorious examples of architectural and structural applications stemming from the various historical periods through the Hellenistic, Byzantine, Knights' and Ottoman periods until nowadays. The preservation of important remnants and historic monuments has permitted sampling and evaluation of historic mortars, even of restoration mortars from the major Italian conservation intervention of the period between World Wars.

Historic mortars are composite materials, comprised of hydraulic or aerial binding material, or a mixture of binding materials, aggregates – not always in crystalline form – and additives, passive or active, which react with the binding material and

* Correspondence and reprints: amoropul@central.ntua.gr

Table I. Sampling[a].

Sample/kind	Location	Historic period of construction
K2: joint mortar	building in Pythagora str. north arch	Knight's 1st period
K3: joint mortar	building in Pythagora str. North orifice	Knight's 1st period
19P: joint mortar	St. Katherine's Hospice	Knight's 1st period
32: joint mortar	Knight's walls opposite to the sea	Knight's 1st period
34: joint mortar	Knight's walls-Carreto bastion, moat	Knight's 2nd period
36: joint mortar	Knight's walls west bastion, Provigia	Knight's 2nd period
4 A: lining mortar external	cistern, centre of the medieval city	Hellenistic Period
4 B: lining mortar internal	cistern, centre of the medieval city	Hellenistic Period
1c: rendering with crushed brick	St. Katherine's Hosp., W wall base, outside	Byzantine period 14th c.
6c: rendering with crushed brick	St. Katherine's Hosp., W wall base, outside	Byzantine period 14th c.
8: lining with crushed brick	St. Katherine's Hospice, roof lining mortar	Byzantine period 6th–8th c.
18: lining with crushed brick	St. Katherine's Hospice, roof lining mortar	Ottoman period 16th–19th c.
13: plaster, internal	St. Katherine's Hospice, int. south wall	Ottoman period 16th–19th c.
9: plaster, internal	St. Athanasios Bastion, duct drain	Knight's 2nd period
7ms: rubble masonry mortar	St. John's Bastion, middle height	Knight's 2nd period
10ms: rubble masonry mortar	St. John's Bastion, from the top	Knight's 2nd period
13ms: rubble masonry mortar	St. Athanasios Bastion, from the base	Knight's 2nd period
15ms: rubble masonry mortar	St. Athanasios Bastion, from the top	Knight's 2nd period
19ms: rubble masonry mortar	Byzantine church, Agisandrou str.	Modern cement-lime restoration mortar

[a] Knight's 1st period: 14th–15th c. (up to 1470 A.D.); Knight's 2nd period: 1470 A.D.–1522 A.D.).

are modified during their setting, hardening and ageing, according to processes as yet not well known [2].

Historic composites concern 'disturbed' systems, as in 'service' for tens of centuries under severe mechanical and environmental loadings. Therefore, the characterization of such materials can be achieved by integrating properly [3] the results of various methods of analysis [4, 5], in order to understand the procedures employed to produce the final composites and the nature of the physico-chemical bonds developed among its constituents.

In the present work the different mortar technologies are investigated aiming to answer questions regarding their finality, i.e. whether their differences arise mainly from the various historical periods of construction or from the purposes they served, imparting to the mortars the properties required by their function in the structure.

The investigation into the various historic mortar technologies is concerned with the determination of the technological parameters which diversify the properties of the final material.

The old city of Rhodes could act as an exemplary case for the purposes under study because the raw materials are allocated to the islands' area and their variety is limited; the various structures of the old city are characteristic of the historical periods; the mortars serve various purposes in the structures, according to their use as joint, rubble masonry or isolating, lining mortars.

2. Experimental methods

2.1. Sampling

With reference to the characteristic historical periods of the city of Rhodes, sampling was carried out on mortars from historical constructions, masonry and architectural surfaces, from both the interior and exterior of the buildings, and serving various structural and architectural uses. *Figure 1* shows the plan of the medieval city of Rhodes with the corresponding sampling locations. *Table I* reports the samples and kinds of mortars, per location, historical periods of construction and use.

2.2. Analysis

2.2.1. Gradation

In order to obtain information on single components and their grain size distribution, some of the mortar samples were fractionated and sieved

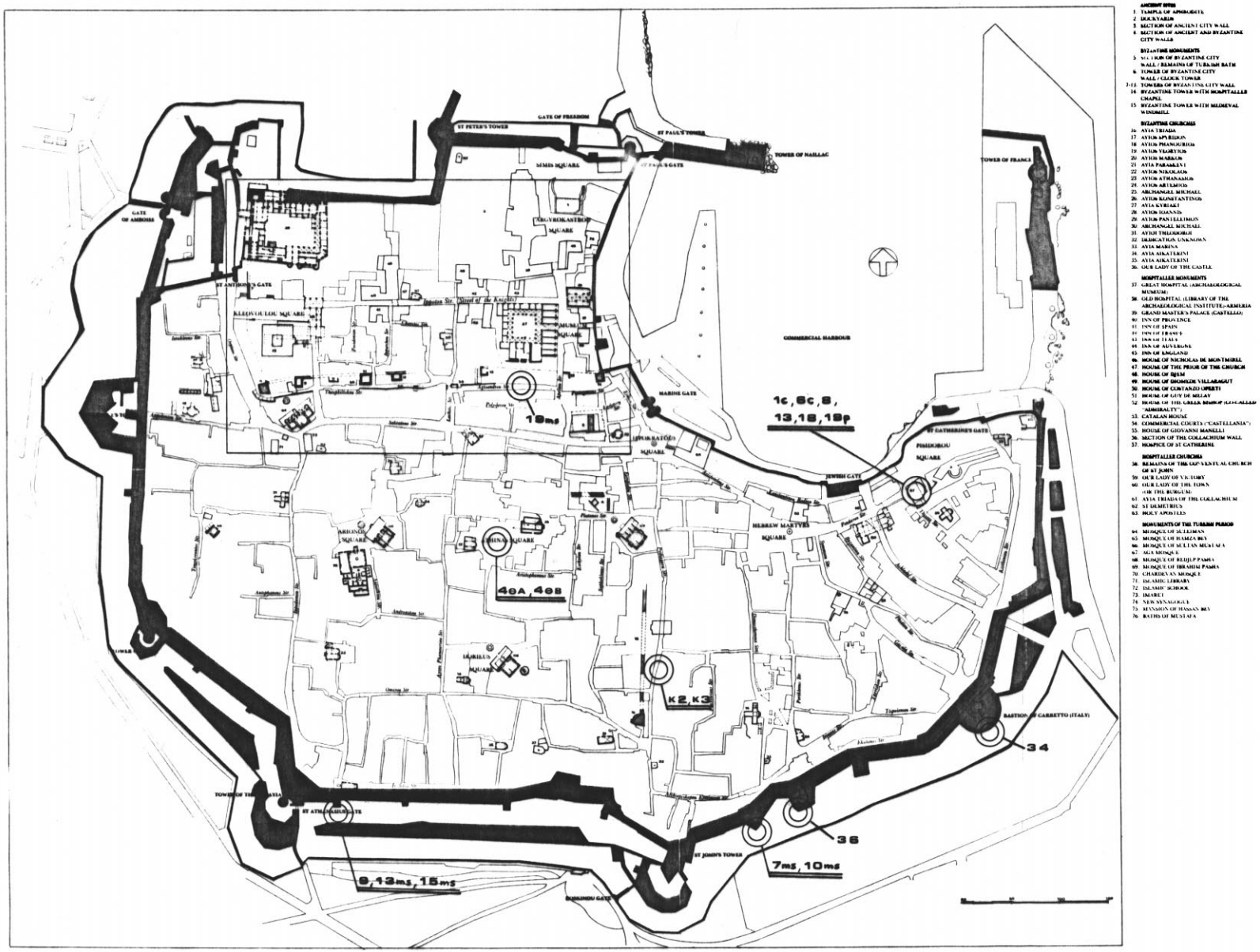

Figure 1. Plan of the medieval city of Rhodes — Sampling locations.

Table II. XRD results[a].

Sample	Composition
K2	calcite, quartz, dolomite
K3	calcite, quartz, dolomite, plagioclase
19p	calcite, quartz, dolomite, plagioclase, leucite
32	calcite, quartz, plagioclase, tobermorite, Halite
34	portlandite, calcite, quartz, chlorite, calcium aluminium hydrate
36	calcite, quartz, dolomite, plagioclase, gypsum
4 a	calcite, quartz, dolomite, plagioclase, gypsum, chlorite, calcium silicium hydrate
4 b	calcite, quartz, dolomite, plagioclase, gypsum, chlorite, calcium silicium hydrate
1c	calcite, quartz, plagioclase, calcium silicium hydrate, calcium aluminium chlorite hydrate, calcium orthosilicate hydrate, montmorillonite
6c	calcite, quartz, dolomite, plagioclase, muscovite, calcium orthosilicate hydrate, tobermorite
8	calcite, quartz, plagioclase, calcium silicium hydrate, muscovite
18	calcite, quartz, plagioclase, calcium silicium hydrate, muscovite
13	calcite, quartz, plagioclase, Halite
9	calcite, quartz, plagioclase, tobermorite, calcium silicium hydrate
7	calcite, dolomite, quartz, plagioclase, muscovite, portlandite, anthophyllite, antigorite, serpentine
10	calcite, quartz, dolomite, muscovite, plagioclase, chlorite, portlandite, anthophyllite, serpentine
13	calcite, quartz, dolomite, muscovite, serpentine, portlandite
15	calcite, quartz, dolomite, aragonite, plagioclase, leucite
19	calcite, dolomite, quartz, anhydrite, yoderite, tobermorite, portlandite

[a] Calcite: $CaCO_3$ (5-0586); quartz: SiO_2 (5-0490); dolomite: $CaMg(CO_3)_2$ (11-78); gypsum: $CaSO_4{\cdot}2H_2O$ (6-46); plagioclase: $CaAl_2Si_2O_8$-$NaAlSi_3O_8$; chlorite: Mg-Fe-Al-Si-O-OH (12-243); calcium aluminium chlorite hydrate: $Al_2O_3CaCl_2.3CaO.10H_2O$ (2-81); muscovite: K,NaAl,Mg,FeSiAlOOH (7-32); yoderite: $Mg_2CaO.2FeO{\cdot}5Al_{5.3}Si_4O_{17.6}(OH)_{2.4}$ (12-625); serpentine: $Mg_3Si_2O_5(OH)_4$ (9-444); calcium silicium hydrate: $5Ca_2SiO_4{\cdot}6H_2O$ (3-0248); montmorillonite: $(AlMg)Si_4O_{10}(OH)_2Na$ (13-259); friedelite: $(Mn,Fe)_8(Si_6O_{15})(OH,Cl)_{10}$ (12-250); portlandite: $Ca(OH)_2$ (4-733); leucite: $KAlSi_2O_6$ (15-47); calcium orthosilicate hydrate: $10CaO.5SiO_2{\cdot}6H_2O$ (3-247); tobermorite: $Ca_5Si_6O_{17}+5H_2O$ (10-373); calcium aluminium hydrate (2-0083); anthophyllite: $(Mg,Fe)_7Si_8O_{22}(OH)_2$ (9-455).

through ISO 565 series of sieves. The lowest fraction (<63 μm) is considered as the binder, although more of less significant quantities of finely grained aggregates could sometimes be found in this fraction.

2.2.2. Microstructure

Intrusion mercury porosimetry (Fisons 4000) was used in order to gather information on the microstructural characteristics of the mortars.

SEM analysis, as in the following procedure, was also performed, in order to observe the pore size distribution, as well as the repletion and replenishment mechanisms of the phenomena occurring within the pores.

2.2.3. Mineralogical and chemical analysis

X-ray diffraction analysis (Siemens D-500) of finely pulverized samples was performed in order to identify the mineral crystalline phases of the mortars.

Optical microscopy of thin sections of mortar samples was used for the petrographical–mineralogical characterization of the mortars' constituents, as well as for microscopic observations on the different mineral phases in the matrix.

Scanning electron microscopy (SEM)/energy dispersive analysis (EDX) (Philips 515) was used for microscopic observations of the microstructure and the texture of the mortars and for elementary semi-quantitative analysis.

Infrared spectroscopy (FT-IR, Biorad FTS 40) was used for gathering qualitative information from a chemical point of view on some of the characteristic substances contained in mortar (calcium carbonate, dolomite, calcium and magnesium hydroxides, gypsum, etc.) and the presence of salts (nitrates, sulphates, oxalates, etc.).

Thermal analyses (TG-DTG, Mettler TG 50) were performed to determine quantitatively some compounds revealed by the infrared spectroscopy and XRD analysis and to determine the nature of their binders and inerts by an appropriate analytical procedure. The analyses were performed with a temperature gradient of 10 °C in a static air atmosphere.

3. Results and discussion

Mineralogical analysis results are given in *table II* and in *figure 2*. As shown by the XR-diffraction in *table II*, calcite is the main component of the matrix. An exclusively calcitic matrix is observed at the

polarizing microscope (*figure 2a*, *b*) identifying typical lime mortars, with quartz clastic grains (*figure 2a*), fossils and characteristic oolithic calcitic aggregate grains (*figure 2b*), as well as feldspars and traces of phyllo-silicate minerals (*table II*, samples K2, K3, 19p, 36, 13).

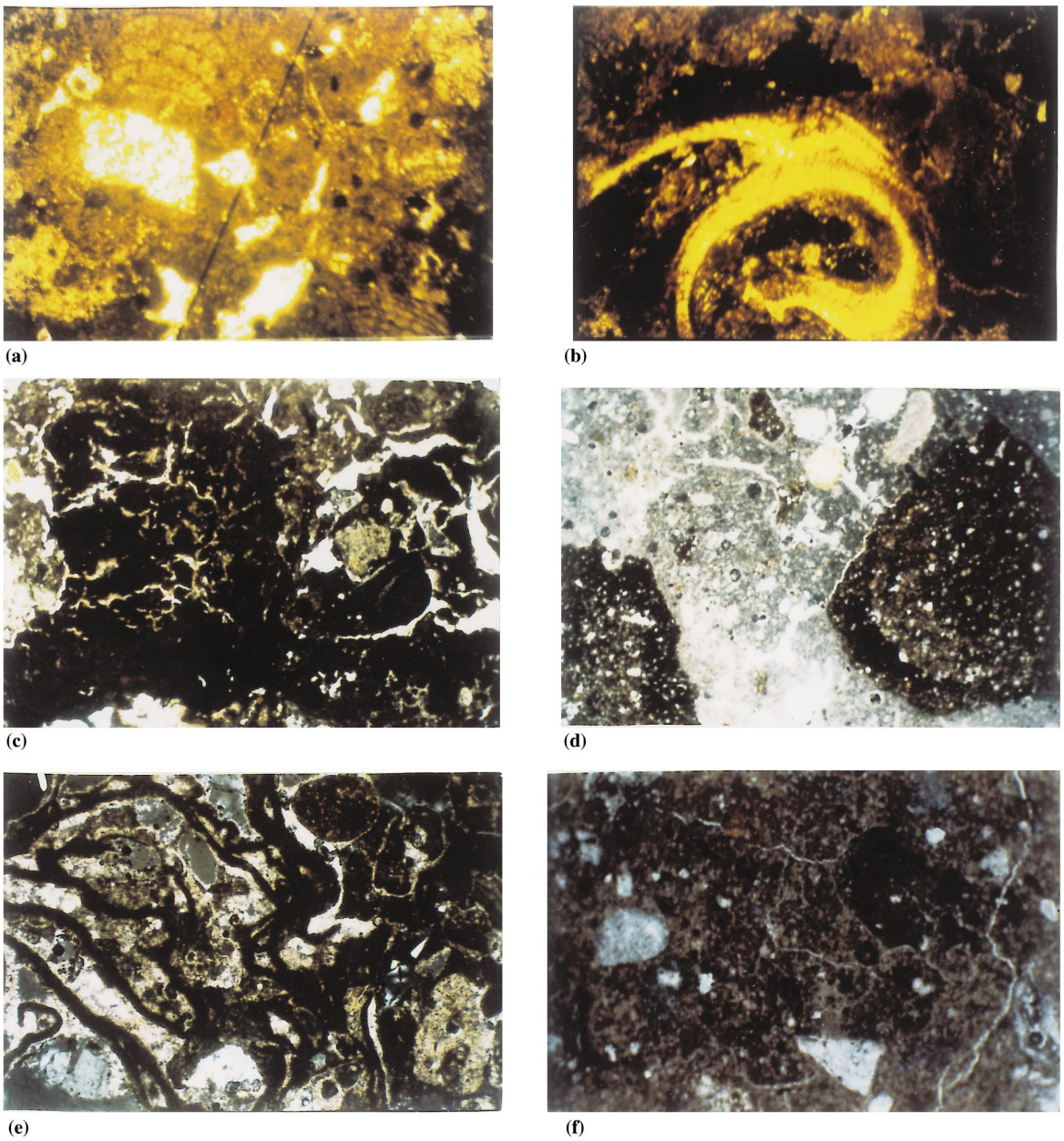

Figure 2. Optical microscopy. a) Microcrystalline calcitic matrix of a typical lime mortar rich in fossils and angle-shaped quartz grains (sample 19P, 40×, #). b) Fossils and oolithic calcitic aggregate grains in the calcitic matrix of a lime mortar (sample k2, 40×, #). c) Crushed brick lining mortars with a characteristic compact matrix (sample 9, 40×, //). d) Ceramic fragments rounded by reaction rims in the matrix (sample 6c, 25×, #). e) Coherent matrix of a rubble masonry mortar embedded by fossils and quartz grains (sample 13ms, 25×, #); f) A fissured compact matrix of a lining mortar, embedded with rounded calcareous and angle-shaped quartz grains (sample 4, 40×, //).

The presence of portlandite, tobermorite and calcium alluminate hydrates (*table II*, samples 32, 34) implies either the use of hydraulic lime or the crystallization of portlandite from lime, when specific construction techniques or environmental conditions are hindering carbonation.

Crushed brick and lime mortars present a characteristic compact matrix (*figure 2c*) traversed by reaction rims (*figure 2d*) at the interfaces between the brick fragments and the calcitic matrix, filling the vacancies and discontinuities of its structure. Fine to medium-grained aggregates are mainly quartz, plagioclase and calcite. Careful observation of the ceramic fragments shows the presence of oxidized, very compact and more or less homogeneous ceramic pieces. The presence of calcium silicate hydrates and calcium aluminate hydrates (*table II*) is significant, indicating interface reactions and/or the presence of the hydraulic lime in the matrix.

Rubble masonry mortars present a coherent matrix embedded with fossils and quartz grains (*figure 2e*). It is a common characteristic of all samples that dolomite and other minerals rich in Mg, such as serpentine, chlorite and anthophilite, are present. Components such as portlandite, montmorilonite and tobermorite are also present in almost all samples. A special characteristic of sample 19 (modern cement mortar) is the presence of yoderite and calcium aluminate chloride hydrate. The XRD results verify the presence of hydraulic components (calcium silicate hydrates, calcium aluminate hydrates, etc.), in almost all samples.

The Hellenistic lining mortar presents a very compact but fissured matrix (*figure 2f*) embedded with rounded calcareous and angle-shaped quartz grains and plagioclase. This image is reminiscent of 'Vitruvius' [6] 'Opus cementicium' or cementitious mortar, which was described as "an artificial conglomerate of gravel with sand and lime cement". However, the XRD identification of calcium silicate hydrates (*table II*) in the matrix along with the historical evidence on the use of pozzolanic material of volcanic provenance for mortar preparation in Rhodes in the ancient years [1] imply a rather pozzolanic mortar.

Hence, different types of matrixes are identified by mineralogical analyses, as confirmed by qualitative chemical analysis (Ft-IR results) [7, 8], and were found to present diversification according to the use of the mortar.

Compact matrixes of very finely crystallized calcite constitute joint mortars of isodomic masonry, its content varying from that of typical lime mortars (exclusively calcitic) to that of hydraulic lime ones.

Cementitious matrixes are provided to serve lining purposes in duct drains, cisterns, wall renderings on near ground level, etc., comprised of crushed brick and lime mortars or pozzolanic ones.

Very coherent and well adhered aggregate matrixes rich in hydraulic components are identified in rubble masonry mortars serving distinctly different purposes to the joint mortars. In the rubble masonry, the mortar constitutes the nucleus of a structural system that is built around it (internal mortar), the strength properties of which depend on the multivariable adhesion bonds built up among mortar–building stone and mortar–aggregate fractals.

However, the aggregates of all mortar types display common features, as they consist mainly of calcite sand, comprised of fine to medium fossils and oolithic aggregate grains, angle-shaped quartz grains and plagioclase. This characteristic permits sieving in order to estimate comparative binder to inert ratios for the various mortar types, since aggregates are inert and do not display hydraulic components, and thermal analysis of the total fraction provides insights into the various mortar matrixes. In the case of thermal analysis of the crushed brick fragments, separation becomes necessary.

Figure 3 shows the grain size distribution of some joint mortars and plasters after fractionation and sieving. Granulometric analysis was performed only on the joint mortars and plasters owing to the great inhomogeneity presented by the rubble masonry mortars because of their specific production technology [9]. Almost all samples present an average of 25 % of binding material in the < 63 μm range. Grain sizes between 63 and 250 μm make up about 40 % of the total for all the samples. A maximum is observed around 250 μm. Then, all the distribution frequencies fall around 500 μm indicating the nature of the mortar aggregates. Only a few fragments are measured with diameters greater than 1 000 μm, above which the fractions tend to zero. The granulometric distribution of the mortars of the medieval city of Rhodes presents a good fit between them and permits the binder/aggregate ratio per volume of the initial mixture to be estimated as 1:3, in respect to of the historical period, mortar type or use served. By these common features the determining role of the mortar aggregates can be defined. This most probably implies the use of sand of the same provenance.

The TG-DTG results from the thermal analysis of 19 samples are shown in *table III* and *figure 4*. *Table III* presents the percentage of weight loss estimated from the TG-DTG curves within the temperature range selected to give important information. Moreover, it reports the water adsorbed

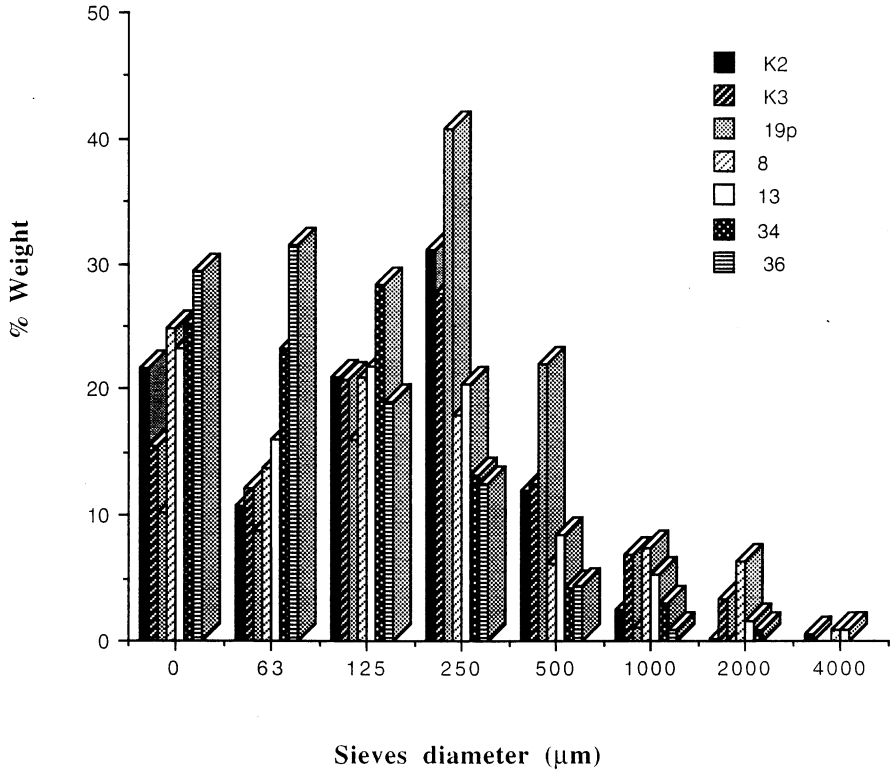

Figure 3. Grain size distribution after sieving.

(hygroscopic water) in the temperature range up to 120 °C, gypsum dehydration between 120 and 200 °C, the structurally bound water to the hydraulic components in the temperature range 200–600 °C, and the calcite decomposition above 600 °C in temperature.

Figure 4 presents the ratio of CO_2/structurally bound water, which inversely expresses the hydraulic character of the mortar in relation to CO_2 (weight loss%). The inverse trend of hydraulicity of the mortar samples is shown to augment exponentially with CO_2.

The following two groups of mortars are discerned.

1) The typical lime mortars correspond to less than 3 % structurally bound water to hydraulic components. In this group, the mortar samples K2, K3, 19p and 13 are included. In the curve, this group corresponds to the area projected at the abscissa in CO_2 values between 33 and 40 % and at the ordinate in CO_2/H_2O ratios above 10.

2) a) The so-called hydraulic mortars include all the categories of mortars with a content of structurally bound water to hydraulic components above 3.5 %, projected at the abscissa in CO_2 values below 30 % and at the ordinate in CO_2/H_2O ratios up to 6. Sample 9, a crushed brick–lime mortar, in the same group of samples as 1, 6, 8 and 18, presents a limiting ratio value of 9, which is in between the hydraulic and the lime mortar area. This is most probably due to the advanced carbonation and deterioration of the mortar as a lining mortar of a duct drain.

b) Two sub-groups could be distinguished between the hydraulic mortars.

– The first group, with a content of structurally bound water to hydraulic components over 10 %, includes the pozzolanic and portlandite mortars – samples 4, 32 and 34 – which present the more advanced hydraulic character. The correspondent curve area is projected at the abscissa in CO_2 values between 10 and 20 %, and at the ordinate in CO_2/H_2O ratio values below 3.5.

– The second group, with structurally bound water to hydraulic components between 3.5 and 6 %, includes crushed brick–lime mortars – samples 1, 6, 8, 13 and 18 – and rubble masonry mortars – samples 7ms, 10ms, 13ms and 15ms. This group

Table III. TG-DTG results.

Samples	Weight loss per temperature range (°C)				
	<120 (%)	120–200	200–600	>600	CO_2/H_2O
K2	0.56	0.47	2.82	33.28	11.80
K3	0.81	0.47	2.99	33.25	11.12
19p	1.25	0.54	2.93	37.14	12.68
32	3.27	3.04	10.51	19.63	1.87
34	1.17	1.55	12.06	18.01	1.49
36	0.97	1.76	6.42	24.34	3.79
4 a	4.46	2.58	15.69	12.35	0.79
4 b	4.14	2.09	15.04	12.87	0.86
1c	1.65	0.94	4.91	27.79	5.66
6c	2.53	0.99	5.20	30.35	5.84
8	1.87	0.62	4.40	25.91	5.89
18	1.04	1.04	4.85	29.92	6.17
13	0.69	0.11	2.02	39.33	19.47
9	1.52	0.50	3.74	33.86	9.05
7ms	2.23	0.47	5.90	19.81	3.36
10ms	1.99	0.41	5.72	23.58	4.12
13ms	1.78	0.39	5.61	28.16	5.02
15ms	1.69	0.37	5.75	29.52	5.13
19ms	2.75	0.91	5.51	9.34	1.69

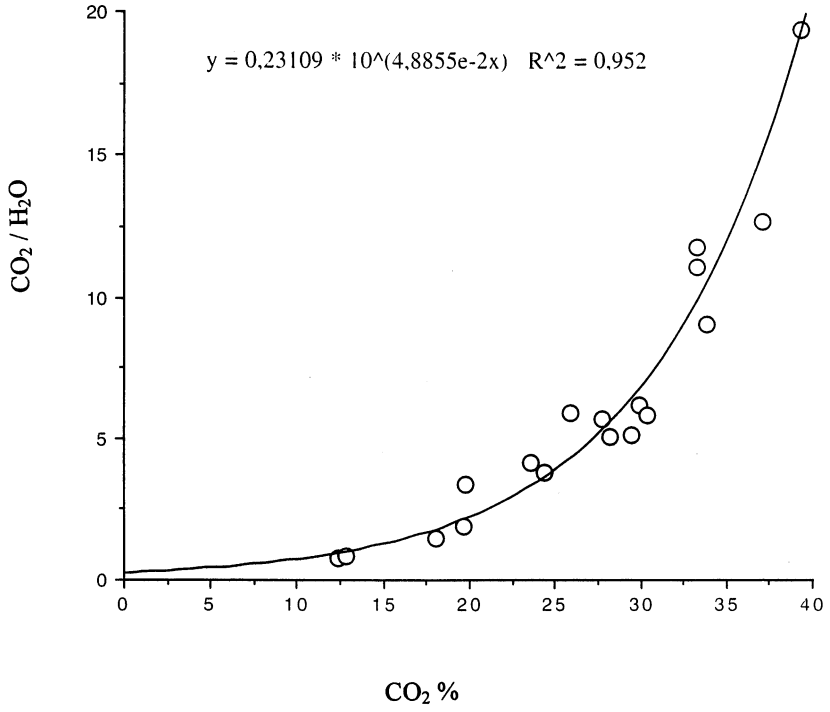

Figure 4. Ratio of CO_2/H_2O versus CO_2%.

Table IV. Microstructural characteristics – results of the porosimetric measurements[a].

Sample	Pv	P%	Rm	As	ã
K2	269.2	43.9	0.39	2.83	1.63
K3	161.2	28.5	19.98	1.47	1.77
34	104.8	19.9	0.03	10.63	1.90
36	241.1	43.4	19.89	1.67	1.80
4	313.5	41.7	0.01	34.49	1.33
8	271.9	42.7	0.39	5.04	1.57
18	194.3	26.0	0.07	7.10	1.34
13	171.1	29.9	0.52	3.27	1.75
7ms	219.8	39.3	0.25	3.48	1.79
10ms	167.1	33.6	19.87	1.90	2.01
13ms	169.4	35.9	20.61	1.22	2.12
15ms	116.9	24.8	20.28	4.66	2.12
19ms	92.5	19.4	0.25	2.38	2.10

[a] Pv: total cumulative volume ($mm^3 \cdot g^{-1}$); P%: total porosity; ã: apparent density ($g \cdot cm^{-3}$); As: specific surface area ($m^2 \cdot g^{-1}$); Rm: medium pore radius (μm).

presents intermediate hydraulic character. The correspondent curve area is projected at the abscissa in CO_2 values between 20 and 30 %, and at the ordinate in CO_2/H_2O ratio values between 3.5 and 6.

c) The modern restoration mortar (sample 19ms) presents a higher level of hydraulicity and is defined at the bottom of the curve with co-ordinates 1.69, CO_2/H_2O ratio, and 9.34 % value, completely diversified from the group containing the historic rubble masonry mortar samples.

The exponentially declining function of the ratio CO_2/H_2O structurally bound (y) to the CO_2 content (x), as expressed by the curve in *figure 4* ($y = 0.23109*10^{(4.8855e-2x)}$ $R^2 = 0.952$), shows a continuous evolution of the kinetics governing the various mechanisms of carbonation of the binder or the formation of hydraulic components during setting, hardening and ageing of the mortars. Hence, the grouping of mortars into well-distinct 'hydraulic levels' should be attempted in relation to the physico-chemical cohesion and adhesion bonds developed at the matrix interfaces.

SEM observations and chemical micro-analyses provide further evaluation criteria. Co-ordinating the results of mortar classification second to cohesion and adhesion bonds, with the results of classification according to the integrated thermal-mineralogical analysis, it was found that the investigated mortars are discerned in the following categories.

3.1. Typical lime mortars

Thermal analyses show the absence of any important weight loss before the calcite decomposition releasing over 33 % CO_2 (equivalent to more than 68 % $CaCO_3$). The binding material is finely crystallized calcite (*figure 5a*), totally carbonated. In lime renderings organic fibres, such as animal hair, were traced as reinforcements to the calcitic matrix (*figure 5f*). The presence of finely crystallized calcite indicates a rather high, almost total, conversion of calcium hydroxide ($Ca(OH)_2$) into calcium carbonate ($CaCO_3$) by atmospheric CO_2, and agrees with the good tensile strength measured (f_{mt}, $k \sim 0.35$ MPa) [10]. The rather high rate of carbonation is attributed to a construction technique that uses thin layers of joints partially covering the porous stone. The humid environment facilitates CO_2 diffusion (above 65 % of relative humidity). Only when the permanent humidity is extremely high (above 80 %), as, for example, in the Caretto Tower – due to the Roman sanitation works – then the carbonation is inhibited and portlandite crystals are observed (*figure 5b*). Protection of mortar joints by marble powder assures the result. In the case of mortars with portlandite crystals, where carbonation is inhibited, structures of a higher density and strength result (*table IV*). However, in that case, two main peaks are observed, that of portlandite (460 °C) and that of calcite (780 °C). Hence, this type of mortar should be classified in the category of highly hydraulic mortars, as confirms its grouping at the bottom of the curve of the inverse trend of hydraulicity in *figure 4*.

3.2. Crushed brick–lime mortars

Among the great variety of traditional mortars, crushed brick mortars are of specific interest owing to their elevated bearing capacity (f_{mt}, $k > 0.55$ MPa). The specific hydraulic character of the crushed brick–lime mortar is attributed to the adhesion reactions occurring at the ceramic–matrix interface (*figures 5c* and *6c*), their nature depending both on the dimensions and type of ceramic (raw materials, clays and firing temperature) and the calcium hydrate content of the mortar. The grain and fragment size of the crushed brick directly influences its hydraulic reactivity, as well as its physico-mechanical properties. The observed reactions could probably be ascribed to the calcium silicate formations at the interface along the brick fragment, acting as the silicate source and membrane and the lime, which makes the interfacial surface alkaline and causes chemical reaction. The penetration of lime into the ceramic and the consequent reaction transforms the microstructure of the ceramic by shifting the pore radii into smaller pores [11]. This

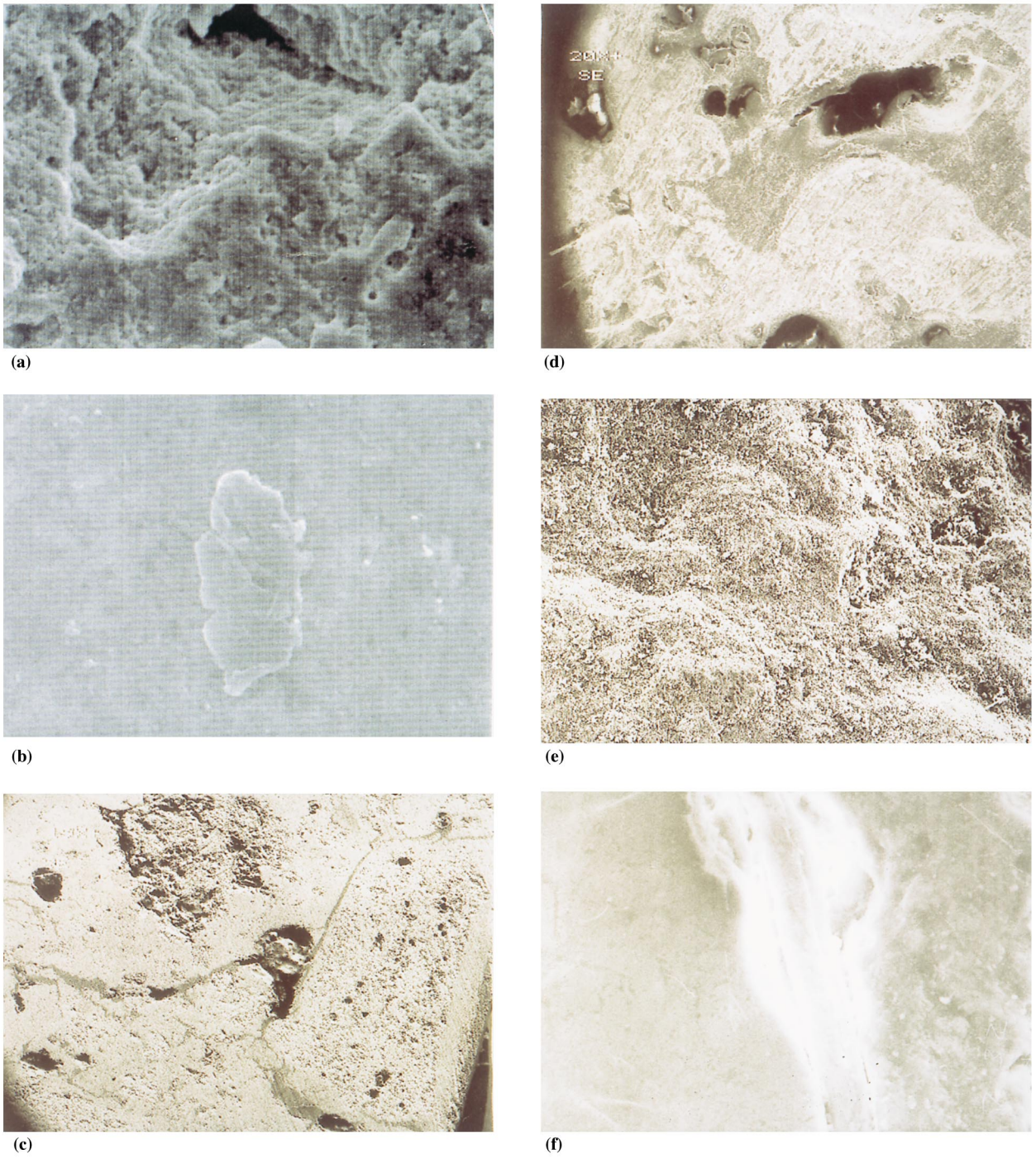

Figure 5. Scanning electron microscopy: observations of mortar samples with regards the study of adhesion and cohesion bonds. a) Fine-crystalline calcitic matrix of a joint mortar (sample 36, 680 ×). b) Portlandite crystal in a coherent matrix of a joint mortar (sample 34, 1 420 ×). c) Reaction rims at the ceramic fragment/matrix interface of a crushed brick–lime lining mortar (sample 1c, 190 ×). d) Two phases of carbonation in the cementitious matrix of a rubble masonry mortar (sample 13ms, 200 ×). e) Fine-grained hydraulic matrix of an Hellenistic lining mortar (sample 4, 930 ×). f) Organic fibre to strengthen a lime plaster (sample 13, 710 ×).

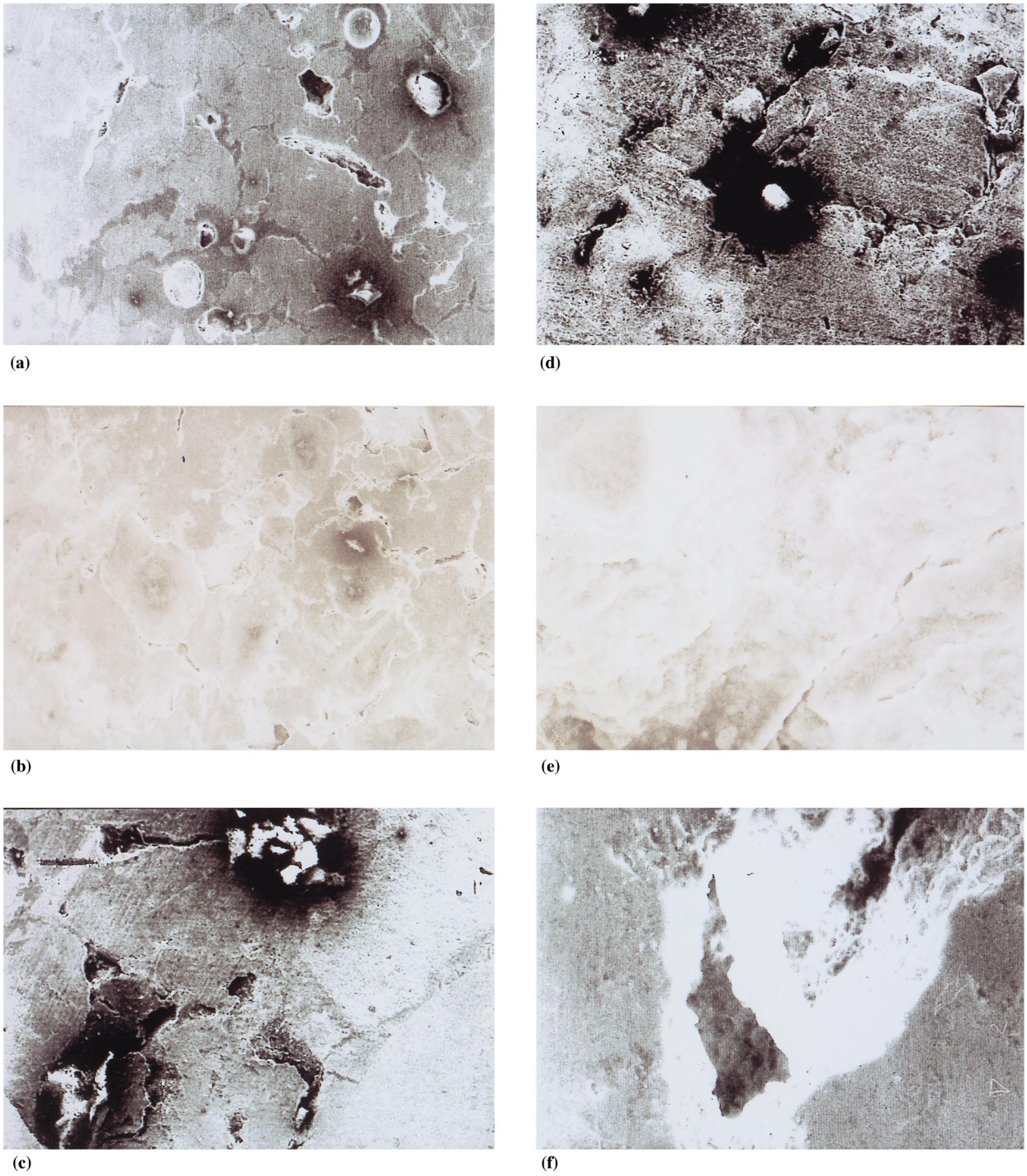

Figure 6. Scanning electron microscopy: observations of mortar samples regarding the study of microtextural characteristics. Characteristic observations of the porosity of: a, b) typical lime joint mortars (a: sample 36, 89×, b: s. K2, 44×); c) crushed brick–lime mortars (sample 8, 490×); d) rubble masonry mortars (sample 10, 13, 420×). Within the pores, either: e) the carbonation of lime to calcite occurs resulting in secondary fine grained calcite (sample 36, 1 420×), or f) salt crystallization of sodium chloride takes place deteriorating the calcitic matrix (sample 36, 356×), or c, d) gypsum formation occurs within the pores of the hydraulic matrix.

transformation matches with the hydraulic character of the mortar matrix, imparting to the mortar high physico-chemical resistance to polluted and marine atmosphere, as well as high strength [12].

3.3. Rubble masonry mortars

Various types of rubble masonry mortars have been demonstrated [9], all of them consisting of hydraulic lime, presenting a very coherent cementitious compact matrix. From the bottom to the top of the masonry, different textural and microstructural characteristics indicate different lime/aggregate ratios and lime stratification, which indicates various carbonation and drying levels (*table IV*). The successive supply of lime to the rubble masonry explains the stratification of the more or less condensed zones, since the aggregate sediments in the lime putty create a white band of hardened matrix (*figure 5d*).

In situ slaking of lime, as an exothermic reaction, gives rise to relatively high temperatures, which in the high alkaline environment provide the energy required to activate reactions for the production either of hydraulic neo-formations or of crystalline compounds, such as portlandite [13]. This technology explains the different carbonation and drying levels, i.e. the higher carbonation at the outer and top of the masonry and the more cementitious matrix in the mortar nucleus near to the ground owing to successive watering and the higher temperatures evolved and retained in the bulk.

Hence, the crystalline portlandite and the hydraulic components formed consequently render in the mortar nucleus dense pore structures imparting high strength and adhesion to the rubble masonry (f_{mt}, k ~ 0.65 MPa).

3.4. Cementitious mortars

The view that basic silicates are formed by burning and then hydrolysed by water yielding lime and hydrated silicates was propounded by A. Winkler and has since been fully established [14]. In the case under study Hellenistic cement mortars present these features. The sequence of small–medium fragments along with the hydraulic components observed by optical microscopy (*figure 2e*) explain the adherence and coherence observed by scanning electron microscopy (*figure 5e*).

Hence, it becomes evident that the determining parameters to diversify the resulting mortar/matrix types are the raw materials employed as binding materials and the production processing. Different cohesion and adhesion bonds allow the mortars to either bear continuous stresses and strains as joint mortars or provide compact impermeable renderings which harden even more on contact with water.

However, mortars and plasters are single constituents of a composite system, and hence, their interaction and compatibility with the building units, stones or bricks are required.

Since no brick is used as a building unit in the cases under investigation, the physico-chemical interaction could not be propounded. The prevailing building stone in Rhodes is a very porous biocalcarenite. Hence, the microstructural characteristics of the mortars and plasters are critical to assure compatibility. The results of the microstructural investigation of the mortar samples are shown in *table IV*.

The porosity of all the mortars varies between 20 and 45 %, as does that of the building units [15].

The only diversification between lime and hydraulic mortars is that in the case of the latter, regression analysis shows a good correlation between specific surface area and the content of structurally bound water to the hydraulic components, with a correlation coefficient of 0.95 [16]. The decrease of pore radii with elevated levels of hydraulicity is well expected [17].

At the upper end, the very dense structure of the modern cement restoration mortar along with the very small pore radii proves that incompatibility with the building units could be a major cause of deterioration. In fact, cement restoration mortars preferentially orientate salt solutions towards the building stones triggering their intense corrosion by salt decay (*figure 7*).

In general, the porosity and pore structure depend on the grain size of the matrix and the binder/aggregate arrangements. Hence, in typical lime mortars (*figure 6a*, *b*) the size and distribution of pores is ascribed to the carbonation rate and to the resulting calcite crystal dimensions, as well as to those of the aggregates. Within the pores, either the carbonation of lime to calcite occurs resulting in secondary fine-grained calcite (*figure 6e*) or salt crystallization of sodium chloride takes place with the deterioration of the calcitic matrix as a consequence (*figure 6f*), or gypsum formation occurs within the pores of the hydraulic matrix (*figure 6c*, *d*).

Environmental deterioration of lime mortars is also attributed to the chemical dissolution of the active microcrystalline binding calcite. When the pore structure is adequate, i.e. micro and macro pores coexist, then salt decay is preferable [15]. Regarding hydraulic mortars, such as crushed

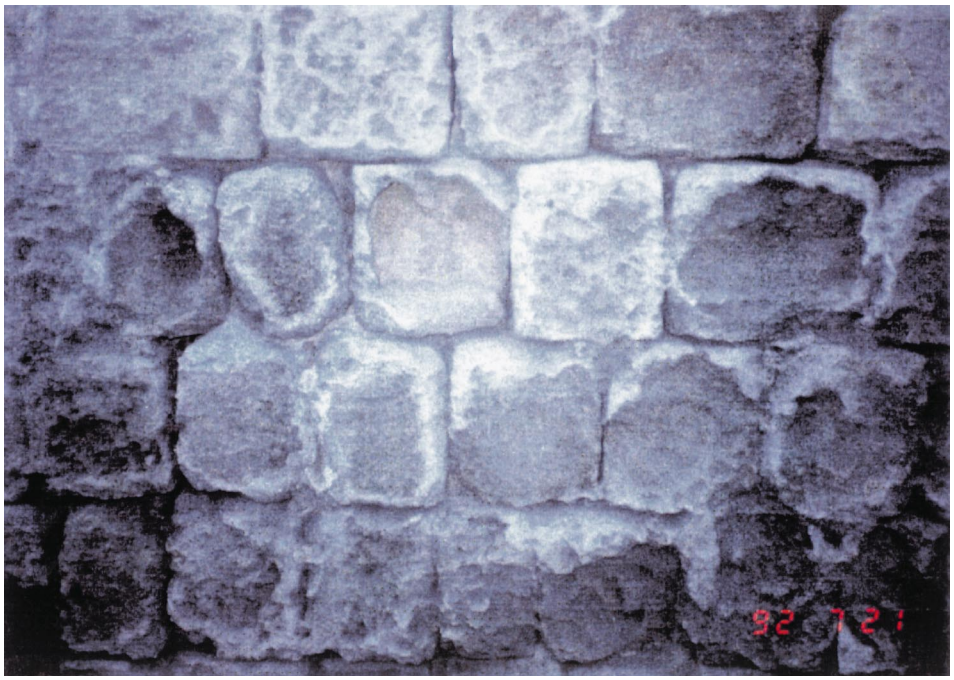

Figure 7. Incompatible modern cement restoration mortars trigger intense corrosion of the porous building stones by salt decay. Detail of the masonry near the Sea Gate of the fortifications.

brick–lime mortars, weathering proceeds with gypsum formation within the pores (*figure 6c*, *d*).

However, pore structure in both categories of mortars, lime or hydraulic ones, presents more or less the same patterns, as shown by the comparison of *figure 6a*, *c*, *d*, highlighting the role of the common aggregates. In contrast, microstructural variations, even within the same group of mortars, might be observed if some production processing parameters are changed, for instance the water content of rubble masonry mortars from bottom to top (samples 7, 10, 13, 15, *table IV*).

4. Conclusions

The granulometric distribution of the various mortars of the medieval city of Rhodes presents a good fit between them and permits the binder/aggregate ratio per volume of the initial mixture to be estimated as 1:3, in respect to the historic period, the mortar type or the function. By these common features the determining role of the mortar aggregates can be defined, most probably implying the use of sand of the same provenance. Aggregates consist mainly of calcite sand, comprised of fine to medium fossils and oolithic aggregate grains, angle-shaped quartz grains and plagioclase. Thermal analysis discerns the group of typical lime to that of hydraulic mortars, including pozzolanic and portlandite ones, with advanced hydraulicity, and crushed brick–lime and rubble masonry mortars with intermediate hydraulicity. The exponentially declining function of the ratio CO_2/H_2O structurally bound to the CO_2 content shows a continuous evolution of the kinetics governing the various mechanisms of carbonation of the binder or the formation of hydraulic components during setting, hardening and ageing of the mortars. The grouping of mortars into well-distinct 'hydraulic levels' is ascribed to the physico-chemical cohesion and adhesion bonds developed at the matrix and matrix/aggregate interfaces, respectively, allowing for the mortars to either bear continuous stresses and strains as joint mortars or provide compact impermeable renderings which harden even more on contact with water. Hence, parameters determining the diversification of the resulting mortar/matrix types concern the raw materials employed as binding materials and the production processing. The microstructural characteristics of the mortars and plasters are critical to assure compatibility. The very dense structure of the modern cement restoration mortar with very small pore radii proved to be

incompatible with the building units, triggering their intense corrosion by salt decay.

Acknowledgements. Acknowledgements are attributed to the Ephore of the 4th Superintendance of Byzantine and Post-Byzantine Monuments of Dodecanese, Dr Elias Kollias for his permit and advice regarding sampling of historic mortars and plasters characteristic of important structural and architectural uses through the historic periods, as well as to archaeologist Mrs Mania Michailidou, architect Mrs Katerina Della and chemical engineer Mrs Argiro Theodoraki for performing the sampling. Acknowledgements are also attributed to the research team of Professor Emeritus Mr Theodosios Tassios and civil engineers Mr M. Chronopoulos and Mr Ch. Spanos, who performed the fragment test on the samples to provide insights on the mechanical strength of the mortar samples.

References

[1] Efstathiadis E., Greek concrete of three millenniums, Technical Report, Research Center of the Hellenic Ministry of Public Works, Athens, Greece, 1978.

[2] Chiari G., Santarelli M.L., Toracca G., Caratterizzazione delle malte antiche mediante l'analisi di campioni non frazionati, Materiali e Strutture 3 (1992) 111–137.

[3] Moropoulou A., Bakolas A., Bisbikou K., Characterization of ancient, byzantine and later historic mortars by thermal analysis and X-ray diffraction techniques, Thermochimica Acta 269/270 (1995) 779–795.

[4] Adams J.E., Kneller A.W., Thermal Analysis of Medieval Mortars from Gothic Cathedrals in France. Engineering Geology of Ancient Works, Monuments and Historical Sites, Balkema, Rotterdam, 1988, pp. 1019–1026.

[5] Charola A.E., Dupas M., Sheryll P.R., Freund G.G., Characterization of ancient mortars: Chemical and instrumental methods, Ed. Ar., Florence, 1984, pp. 28–33.

[6] Vitruvius P., The Ten Books on Architecture, Trans. M.H. Morgan, Dover Publications, New York, 1960.

[7] Moropoulou A., Biscontin G., Bisbikou K., Bakolas A., Theoulakis P., Theodoraki A., Tsiourva T., Zendri E., 'Opus caementicium' mortars in a polluted and marine atmosphere: behaviour patterns distinct to cement and lime mortars, Scienza e Beni Culturali IX, Publ. Libreria Progetto Editore, Padova, Italy, 1993, pp. 357–371.

[8] Moropoulou A., Biscontin G., Bakolas A., Bisbikou K., Theoulakis P., Theodoraki A., Zendri E., Physicochemical investigation on characterisation and behaviour of rubble masonry mortars 'Calcestruzzo da Sacco Murario', Scienza e Beni Culturali IX, Publ. Libreria Progetto Editore, Padova, Italy, 1993, pp. 373–387.

[9] Doglioni F., Bellina A., Bona A., Biscontin G., Cusinato G., Volpin S., Driussi G., Ricerca sulle tecnologie storiche di costruzione e manutenzione del Duomo di S. Andrea Ap. A Venzone (UD): Le malte di sacco murario, Scienza e Beni Culturali XII, Publ. Libreria Progetto Editore, Padova, Italy, 1996, pp. 571–595.

[10] Moropoulou A., Biscontin G., Theoulakis P., Bisbikou K., Theodoraki A., Chondros N., Zendri E., Bakolas A., Study of mortars in the Medieval City of Rhodes, in: Proc. Unesco-Rilem Int. Congress on Conservation of Stone and Other Materials, Unesco, Paris, 1993, pp. 394–401.

[11] Moropoulou A., Cakmak A.S., Biscontin G., Crushed brick lime mortars of Justinian's Hagia Sophia, in: Materials Issues in Art and Archaeology V, Publ. Materials Research Society, 1996.

[12] Moropoulou A., Biscontin G., Bisbikou K., Bakolas A., Theoulakis P., Theodoraki A., Tsiourva T., Physicochemical study of adhesion mechanisms among binding material and brick fragments in "Coccio Pesto", Scienza e Beni Culturali IX, Publ. Libreria Progetto Editore, Padova, Italy, 1993, pp. 415–429.

[13] Moropoulou A., Biscontin G., Bakolas A., Bisbikou K., Technology and behavior of rubble masonry mortars, Construction and Building Materials 11 (1997) 119–129.

[14] Winkler A., Hydrated lower silicates yielded by hydrolysis of basic silicates, Praktische Chemie 67 (1856) 444.

[15] Theoulakis P., Moropoulou A., Microstructural and mechanical parameters determining the susceptibility of porous building stones to salt decay, Construction and Building Materials 11 (1997) 65–71.

[16] Bassiotis I., Correlation of physico-chemical and mechanical characteristics of historic mortars in the Mediterranean, thesis, National Technical University of Athens, Greece, 1996.

[17] Schafer J., Hilsdorf H.K., Ancient and new lime mortars – The correlation between their composition structure and properties, in: Proc. Unesco-Rilem Int. Congress on Conservation of Stone and Other Materials, Unesco, Paris, 1993, pp. 605–613.